Physica B 404 (2009) 1558–1562

Contents lists available at ScienceDirect

Physica B

journal homepage: www.elsevier.com/locate/physb

# Temperature-dependent current–voltage characteristics of the Au/*n*-InP diodes with inhomogeneous Schottky barrier height

F.E. Cimilli [a], M. Sağlam [a], H. Efeoğlu [b], A. Türüt [a,*]

[a] Faculty of Sciences and Arts, Department of Physics, Atatürk University, 25240 Erzurum, Turkey
[b] Faculty of Engineering, Department of Electric and Electronics Engineering, Atatürk University, 25240 Erzurum, Turkey

ARTICLE INFO

*Article history:*
Received 2 January 2009
Received in revised form
13 January 2009
Accepted 14 January 2009

*Keywords:*
Schottky barrier inhomogeneity
*n*-InP semiconductor
Schottky diodes

ABSTRACT

The current–voltage (*I–V*) characteristics of Au/*n*-InP Schottky contacts have been measured in the temperature range of 70–300 K by steps of 10 K. Our data of the Au/*n*-InP Schottky contact strongly suggest that the temperature-dependent electron transport at the metal–semiconductor interface is significantly affected by the barrier inhomogeneity. The distribution of local effective SBHs has been modeled by a summation of existence of double Gaussian barrier heights which represents the high- and low-barrier of the full distribution in 170–300 and 70–170 K ranges.

© 2009 Elsevier B.V. All rights reserved.

## 1. Introduction

The wide band-gap III–V compound semiconductors due to the fabrication of various electronic and optoelectronic devices have important applications in the last years. Metal film deposition on InP substrates semiconductor has received much attention for the fabrication of optoelectronics, microwave devices, and integrated circuits used in modern high-speed optical communication system [1–5]. Metal–semiconductor (MS) contact is one of the most widely used rectifying contacts in the electronics industry [2–8]. The current–voltage (*I–V*) characteristics of the MS contacts usually deviate from the ideal thermionic emission (TE) current model [6–15]. There are currently a vast number of reports of experimental studies of characteristic parameters such as the barrier height (BH) and ideality factor in a great variety of MS contacts [15–25]. The popularity of such studies, which is rooted in their importance to the semiconductor industry, does not assure uniformity of the results or of interpretation. Schottky diodes (SDs) with low BH have found applications in devices operating at cryogenic temperatures as infrared detectors and sensors in thermal imaging [14–30]. Therefore, analysis of the *I–V* characteristics of the Schottky barrier diodes (SBDs) at room temperature only does not give detailed information about their conduction process or the nature of barrier formation at the MS interface. The temperature dependence of the *I–V* characteristics allows us to understand different aspects of conduction mechanisms [19–39]. However, a complete description of the charge carrier transport through an MS contact is still a challenging problem.

The BH in Schottky contacts is likely a function of the interface atomic structure, and the atomic inhomogeneities at MS interface which are caused by grain boundaries, multiple phases, facets, defects, a mixture of different phases, etc. [27–40]. Additionally, there may be doping inhomogeneity at the MS interface, dopant clustering. Contamination at the MS interface due to undesirable reaction products or particulates is often present at the MS interfaces of diodes prepared by the routine processing methods used in the semiconductor electronics industries. These contaminants may act directly to introduce inhomogeneity or they may simply promote inhomogeneity, through the generation of defects [26–42]. Apart from the roughness of the interface due to thickness modulations of the metal as well as atomic steps, dislocations, and grain boundaries in the metal, these potential fluctuations may also originate from a local effective barrier lowering due to field emission at metallic diffusion spikes with narrow radii of curvature [26,36,37].

In the present study, the *I–V* characteristics of Au Schottky contacts on an *n*-InP substrate were measured over the temperature range of 70–300 K by steps of 10 K. The temperature-dependent barrier characteristics of the Au/*n*-InP Schottky contacts were interpreted by means of the TE theory of inhomogeneous Schottky contacts suggested by some authors [30–32].

## 2. Experimental procedure

The SBDs were prepared using *n*-type InP (1 0 0) wafer. The carrier concentration values of $2.563 \times 10^{15}$ and $2.594 \times 10^{15}$ $cm^{-3}$

* Corresponding author. Tel.: +90 442 231 4171; fax: +90 442 236 0948.
*E-mail address:* aturut@atauni.edu.tr (A. Türüt).

0921-4526/$ - see front matter © 2009 Elsevier B.V. All rights reserved.
doi:10.1016/j.physb.2009.01.018

for the *n*-type InP wafer were found from the experimental reverse bias $C^{-2}$–$V$ characteristics at 70 and 300 K, respectively. The wafer was degreased consecutively in trichloroethylene, acetone, and methanol for 5 min. The degreased wafer was etched with $H_2SO_4$:$H_2O_2$:$H_2O$ (5:1:1) for 1 min to remove the surface damages and undesirable impurities. The back side ohmic contact was made by evaporating In and annealing at 300 °C in $N_2$ atmosphere for 3 min. The Schottky contacts were formed on the front face of the pieces as dots with diameter of about 1.0 mm by evaporation of Au (diode area = $7.85 \times 10^{-3}$ cm$^2$). All evaporation processes were carried out in a vacuum coating unit at about $10^{-6}$ mbar. The $I$–$V$ and $C$–$V$ characteristics of the devices were measured in the temperature range of 70–300 K using a temperature controlled ARS closed cycle 4 K He cryostat, temperature stability for each run was better than 0.1 K. Keithley 6514 electrometer and 2400 sourcemeter used for $I$–$V$ measurements.

## 3. Results and discussion

### 3.1. Temperature dependence of the forward-bias I–V characteristics

To understand whether or not a SD has the ideal diode behavior we analyze its experimental $I$–$V$ characteristics by the forward-bias TE theory given as follows [2]:

$$I = I_0 \exp\left(\frac{q(V - IR)}{nkT}\right)\left[1 - \exp\left(-\frac{q(V - IR)}{kT}\right)\right] \quad (1)$$

where

$$I_0 = AA^*T^2 \exp\left(-\frac{q\Phi_{eff}}{kT}\right) \quad (2)$$

is the saturation current derived from the straight line intercept of $\ln I$ at $V = 0$, $q$ is the electron charge, $V$ is the forward-bias voltage, $A$ is the effective diode area, $k$ is the Boltzmann constant, $T$ is the absolute temperature, $A^*$ is the effective Richardson constant of 9.8 A cm$^{-2}$ K$^{-2}$ for *n*-type InP [4], $R_s$ is the series resistance of the neutral region of the semiconductor bulk (between the depletion region and ohmic contact), $IR_s$ is the voltage drop across the series resistance, $\Phi_{eff}$ is the experimental zero bias BH (apparent BH) and $n$ is the ideality factor. From Eq. (1), ideality factor $n$ can be written as

$$n = \frac{q}{kT}\left(\frac{dV}{d\ln I}\right) \quad (3)$$

The semilog-forward and reverse bias $I$–$V$ characteristics of the Au/*n*-InP SBDs are shown in the temperature range of 70–300 K by the steps of 10 K in Fig. 1. The experimental values of $\Phi_{eff}$ (apparent BH) and $n$ have been determined from intercepts and slopes of the forward-bias $\ln I$ vs. $V$ plot at each temperature using the TE theory, respectively. That is, $\Phi_{eff}$ and $n$ have been evaluated from the upper part of the temperature-dependent forward-bias $I$–$V$ characteristics from 70 to 240 K. The experimental values of $\Phi_{eff}$ and $n$ for the device range from 0.57 eV and 1.07 (at 300 K) to 0.20 eV and 3.03 (at 70 K), respectively. $\Phi_{eff}$ and $n$ plots as a function of temperature are presented in Fig. 2. In this figure, the values of $n$ are indicated by the open triangles and the values of $\Phi_{eff}$ by the closed triangles. As can be seen in the figure, both parameters exhibit strong temperature dependence. That is, the apparent BH decreased and $n$ increased with a decrease in temperature. Since current transport across the MS interface is a temperature activated process, electrons at low temperatures are able to surmount the lower barriers and therefore, the current transport will be dominated by current flow through the patches of lower SBH and a larger ideality factor. As the temperature increases, more and more electrons have sufficient energy to surmount the higher barrier [35–38].

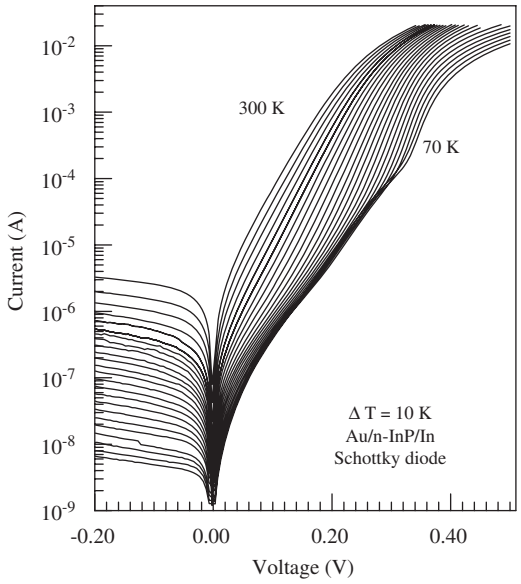



**Fig. 1.** Experimental forward-bias current–voltage characteristics of an Au/*n*-InP/In Schottky contact at various temperatures.

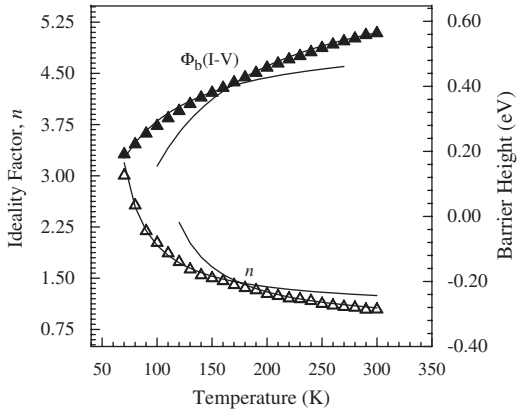



**Fig. 2.** Temperature dependence of the ideality factor (the open triangles) and barrier height (the filled triangles) for Au/*n*-InP/In Schottky diode.

The slope of the activation energy $\ln(I_0/T^2)$ vs. $1/kT$ plot allows the determination of the effective SBH according to Eq. (2). This plot is indicated by the closed triangles in Fig. 3. The significant deviation from linearity of the experimental $\ln(I_0/T^2)$ vs. $1/T$ plot at low temperatures in Fig. 3 demonstrates that the fit of the experimental data is impossible for the determination of the effective SBH, independent of temperature. The significant deviation from linearity of the experimental $\ln(I_0/T^2)$ vs. $1/T$ curve is caused by the temperature dependence of the BH and ideality factor. As will be discussed below, the deviation in the Richardson plots may be due to the presence of the spatially inhomogeneous BHs and potential fluctuations at the interface that consist of low- and high-barrier areas [26,35–39], that is, the current through the diode will flow preferentially through the lower barriers in the potential distribution [26,35–39]. Likewise, the activation energy $\ln(I_0/T^2)$ vs. $1/nkT$ plot (open triangles) with the ideality factors was drawn, and this plot yielded a straight line with an activation energy value of 0.53 eV. This value is in agreement with a homogeneous BH value of approximately 0.524 eV from the

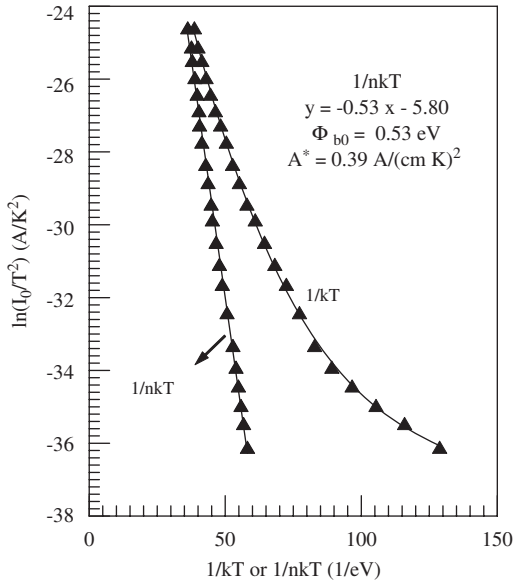



**Fig. 3.** Richardson plots of the $\ln(I_0/T^2)$ vs. $1/T$ plot (the filled triangles) and $\ln(I_0/T^2)$ vs. $1/nT$ plot (the open triangles) for Au/*n*-InP/In Schottky diode.

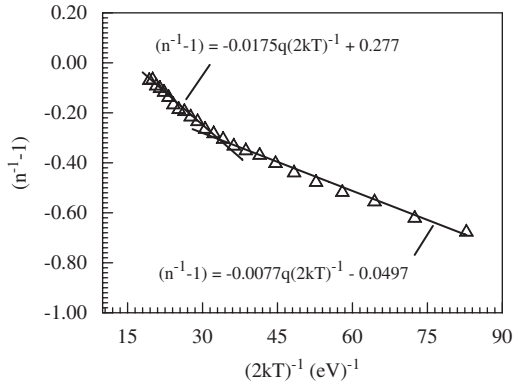



**Fig. 4.** Temperature dependence of the ideality factor for Au/*n*-InP/In Schottky diode. The continuous curves show estimated values of ideality factor using Eq. (5) for two Gaussian distributions of barrier heights with $\rho_2 = -0.277$, $\rho_3 = -0.0175$ V in 170–300 K and $\rho_2 = 0.0497$, $\rho_3 = -0.0077$ V in 70–170 K.

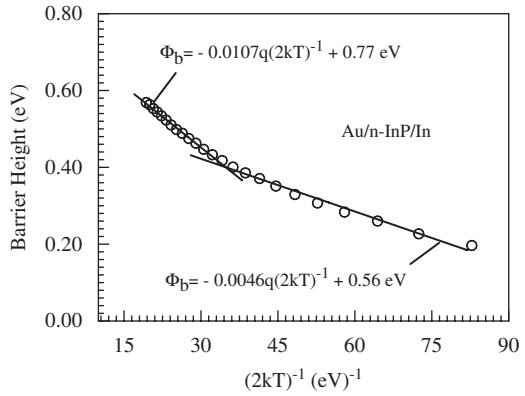



**Fig. 5.** Temperature dependence of and barrier height for Au/*n*-InP/In Schottky diode. The continuous curve related to the filled circles represents estimated values of $\Phi_{ap}$ using Eq. (4) for two Gaussian distributions of barrier heights with $\overline{\Phi}_{bo} = 0.77$ eV and $\sigma_{so} = 103$ mV in 170–300 K and $\overline{\Phi}_{bo} = 0.56$ eV and $\sigma_{so} = 68$ mV in 70–170 K (the curve 1).

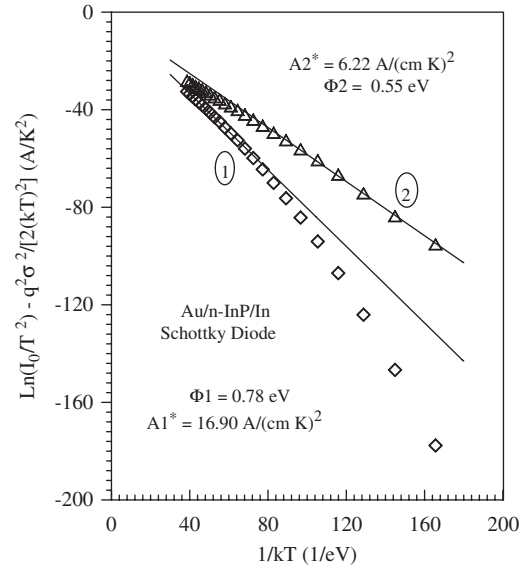



**Fig. 6.** Richardson plot of the $\ln(I_0/T^2)$ vs. $1/T$ plot (the open triangles) and modified Richardson $\ln(I_0/T^2) - q^2\sigma_{so}^2/2k^2T^2$ vs. $1/T$ plot for the Au/*n*-InP/In Schottky diode according to two Gaussian distributions of barrier heights. The open squares represent the plot calculated for $\sigma_{so} = 69$ mV (the straight lines 2) in temperature ranges of 70–170 K and the open triangles represent the plot calculated for $\sigma_{so} = 103$ mV (the straight lines 1) in temperature ranges of 170–300 K.

extrapolation of the experimental SBHs vs. ideality factors plot to $n = 1$ given for Au/*n*-InP SBDs in Ref. [3].

The commonly observed deviation from classical TE theory, as will be discussed below, can be explained by a recent model based on the assumption of a spatial fluctuation of the BH at interface [6–8,19–35]. The continuous curves in Figs. 2,4–6 and the linearity of the ideality factor vs. $1/T$ curve in Fig. 4 show that the temperature dependence experimental data of the Au/*n*-InP Schottky contact are in agreement with the recent model [30–34] which is the related to TE over a Gaussian BH distribution. The BH has a Gaussian distribution with the zero bias mean BH $\overline{\Phi}_{bo}$ [8,10,15–17]. The Gaussian distribution of the BH yields the following expression for the BH [31–33]:

$$\Phi_{ap} = \overline{\Phi}_{bo} - \frac{q\sigma_{so}^2}{2kT} \tag{4}$$

where $\Phi_{ap}$ is the apparent BH measured experimentally and $\sigma_{so}$ is the zero bias standard deviation of the BH distribution. The temperature dependence of $\sigma_{so}$ is usually small and can be neglected. The standard deviation is a measure of the barrier homogeneity. The above expression for the apparent BH construction was used already by Song et al. [30] and also by Werner and Güttler [31]. The observed variation of ideality factor with temperature in the model is given by [31]

$$\left(\frac{1}{n_{ap}} - 1\right) = -\rho_2 + \frac{q\rho_3}{2kT} \tag{5}$$

where $n_{ap}$ is apparent ideality factor, and the coefficients $\rho_2$ and $\rho_3$ quantify the voltage deformation of the BH distribution, that is, the voltage dependencies of the mean BH and the barrier distribution width are given by coefficients $\rho_2$ and $\rho_3$, respectively.

The experimental $n_{ap}$ vs. $1/T$ (Fig. 4) and $\Phi_{ap}$ vs. $1/T$ (Fig. 5) plots drawn by means of the experimental data obtained from Fig. 1 respond to two lines instead of a single straight line with

transition occurring at 170 K. The linearity of the apparent BH or ideality factor vs. $1/T$ curves in Figs. 4 and 5, and the continuous curves in Fig. 2 show that the temperature-dependent experimental data of the Au/$n$-InP Schottky contact are in agreement with the recent model which is related to TE over two Gaussian distributions of BHs in the contact area [12–17]. The values of $\rho_2$ obtained from the intercepts of the experimental $n_{ap}$ vs. 1/T plot are −0.277 in 170–300 K range and 0.0497 in 70–170 K range, whereas the values of $\rho_3$ from the slopes are −0.0175 V in 170–300 K range and −0.0077 V in 70–170 K range. The intercept and slope of the straight line have given two sets of values of $\overline{\Phi}_{bo}$ and $\sigma_{so}$ as 0.77 eV and 103 mV in the temperature range of 170–300 K, and as 0.56 eV and 68 mV in the temperature range of 70–170 K. Furthermore, the $\Phi_{ap}$ and $n_{ap}$ values estimated from Eqs. (8) and (9) over the entire temperature range of 70–300 K using the $\overline{\Phi}_{bo}$, $\sigma_{so}$ and $\rho_2$, $\rho_3$ values obtained for these two regions are shown by the continuous curves in Fig. 2. That is, the continuous solid lines related to the open triangles in Fig. 3 represent the data estimated using Eq. (4). The linear behavior of this plot demonstrates that the ideality factor indeed expresses the voltage deformation of the Gaussian distribution of the Schottky BH. The continuous solid lines in Fig. 2 represent data estimated with the above values of $\rho_2$ and $\rho_3$ using Eq. (5). As can be seen, the computed values exactly coincide with the experimental results in the respective temperature ranges for two different distributions. This is actually clear from the determined values of the mean BH and the standard deviation of distributions 1 and 2 which are given above. In addition to the explanations above, the regions with two different mean BHs exist for all temperatures investigated by us. Thus, it can be indicated that now these two regions have different area ratio. From the data it seems clearly that the total area of regions with the lower mean BH must be lower than that of the regions with higher mean BH. Therefore, we have found that the region with higher BH is dominant for higher temperatures (which would be impossible if the area ratio of regions with different BH was 1, in that case, the region with lower BH would dominate current transport).

The conventional activation energy $\ln(I_0/T^2)$ vs. $1/T$ plot has showed nonlinearity at low temperatures. To explain these discrepancies, according to the Gaussian distribution of the BH, it can be rewritten as

$$\ln\left(\frac{I_0}{T^2}\right)-\left(\frac{q^2\sigma_s^2}{2k^2T^2}\right)=\ln(AA^*)-\frac{q\overline{\Phi}_{bo}}{kT} \quad (6)$$

and a modified activation energy plot from this expression is obtained. Using the experimental $I_0$ data, a modified $\ln(I_0/T^2)-q^2\sigma_{so}{}^2/2k^2T^2$ vs. $1/T$ plot can be obtained according to Eq. (6) and should give a straight line with slope directly yielding the mean $\overline{\Phi}_{bo}$ and the intercept ($=\ln AA^*$) at the ordinate determining $A^*$ for a given diode area $A$. The $\ln(I_0/T^2)-q^2\sigma_{so}{}^2/2k^2T^2$ values were calculated for both two values of $\sigma$ obtained for the temperature ranges of 70–170 and 170–300 K. Thus, the open triangles and open squares in Fig. 6 have given the modified $\ln(I_0/T^2)-q^2\sigma_s{}^2/2k^2T^2$ vs. $1/T$ plots for both two values of $\sigma_{so}$. The best linear fitting to these modified experimental data are depicted by solid lines in Fig. 6 which represent the true activation energy plots in respective temperature ranges. The calculations yielded zero bias mean BH $\overline{\Phi}_{bo}$ of 0.55 eV (in the range of 70–170 K) and 0.78 eV (in the range of 170–300 K). These values match exactly with the mean BHs obtained from the $\Phi_{ap}$ vs. $1/T$ plot in Fig. 5. The intercepts at the ordinate give the Richardson constant $A^*$ as 6.22 A/cm$^2$ K$^2$ (in 70–170 K range) and 16.90 A/cm$^2$ K$^2$ (in 170–300 K range) without using the temperature coefficient of the BHs.

In conclusion, the apparent BH, $\Phi_{bo}$, from the current–voltage ($I$–$V$) characteristics of the Au/$n$-InP Schottky contact decreases while the ideality factor $n$ increases with a decrease in temperature due to the barrier inhomogeneity or to local enhancement of electric field which can also yield a local reduction of the BH. The activation energy $\ln(I_0/T^2)$ vs. $1/nkT$ plot yielded a straight line with an effective BH value of 0.53 eV. It has been seen that under the Gaussian distribution of BH model or $n$ vs. $1/T$ plot shows a two slope behavior and serves as the basis for the proposal of the presence of a double Gaussian distribution of BHs at the MS interface. The modified $\ln(I_0/T^2)-q^2\sigma_{so}{}^2/2k^2T^2$ vs. $1/T$ plots yielded zero bias mean BH $\overline{\Phi}_{bo}$ of 0.56 eV (in the range of 70–170 K) and 0.78 eV (in the range of 170–300 K). These values match exactly with the mean BHs obtained from the $\Phi_{ap}$ vs. $1/T$ plot. The modified activation energy plot from the barrier inhomogeneity model have given the Richardson constant $A^*$ as 16.90 and 6.22 A/cm$^2$ K$^2$. It has been seen that the obtained Richardson constant values are in close agreement with the known value of 9.8 A/cm$^2$ K$^2$ for $n$-type InP.

## References


[1] H. Yan, E. Shunsuke, H. Yusuke, O. Hidenori, Chem. Lett. 36 (8) (2007) 986.
[2] E.H. Rhoderick, R.H. Williams, Metal-Semiconductor Contacts, Clarendon Press, Oxford University Press, Oxford, 1988, p. 20, 48.
[3] H. Cetin, E. Ayyildiz, Semicond. Sci. Technol. 20 (2005) 625.
[4] R.H. Williams, G.Y. Robinson, in: C.W. Wilmsen (Ed.), Physics and Chemistry of III–V Compound Semiconductor Interfaces, Plenum Press, New York, 1985.
[5] R.L. Van Meirhaeghe, W.H. Laflére, F. Cardon, J. Appl. Phys. 76 (1994) 403.
[6] E. Gur, S. Tuzemen, B. Kilic, C. Coskun, J. Phys. Condens. Matter 19 (2007) 196206.
[7] N. Rouag, L. Boussouar, S. Toumi, Z. Ouennoughi, M.A. Djouadi, Semicond. Sci. Technol. 22 (4) (2007) 369.
[8] D.M. Kim, D.H. Kim, S.Y. Lee, Solid-State Electron. 51 (2007) 865.
[9] A.F. Qasrawi, Semicond. Sci. Technol. 21 (2006) 794.
[10] M.M. El-Nahass, H.M. Zeyada, K.F. Abd-El-Rahman, A.A.A. Darwish, Sol. Energy Mater. Sol. Cells 91 (2007) 1120.
[11] Dhananjay, J. Nagaraju, S.B. Krupanidhi, Physica B 391 (2007) 344.
[12] R. Pérez, N. Mestres, J. Montserrat, D. Tournier, P. Godignon, Phys. Stat. Sol. (a) 202 (4) (2005) 692.
[13] A.R. Arehart, B. Moran, J.S. Speck, U.K. Mishra, S.P. Den Baars, S.A. Ringel, J. Appl. Phys. 100 (2006) 023709.
[14] F. Roccaforte, F. La Via, V. Raineri, R. Pierobon, E. Zanoni, J. Appl. Phys. 93 (11) (2003) 9137.
[15] C.F. Pirri, S. Ferrero, L. Scaltrito, D. Perrone, S. Guastella, M. Furno, G. Richieri, L. Merlin, Microelectron. Eng. 83 (2006) 86.
[16] K.V. Vassilevski, I.P. Nikitina, N.G. Wright, A.B. Horsfall, A.G. O_Neill, C.M. Johnson, Microelectron. Eng. 83 (2006) 150.
[17] M. Pattabi, S. Krishnan, Ganesh, X. Mathew, Solar Energy 81 (1) (2007) 111.
[18] F. Yakuphanoglu, Physica B 389 (2) (2007) 306.
[19] S. Kumar, Y.S. Katharria, S. Kumar, D. Kanjilal, J. Appl. Phys. 100 (2006) 113723.
[20] I. Dokme, S. Altindal, M.M. Bulbul, Appl. Surf. Sci. 252 (22) (2006) 7749; I. Dokme, S. Altindal, Semicond. Sci. Technol. 21 (8) (2006) 1053.
[21] F. Brovelli, B.L. Rivas, J.C. Bernede, J. Chilean Chem. Soc. 52 (1) (2007) 1065.
[22] N.L. Dimitruk, O.Yu. Borkovskaya, I.N. Dimitruk, S.V. Mamykin, Zs.J. Horvath, I.B. Mamontova, Appl. Surf. Sci. 190 (2002) 455.
[23] S.W. Kim, K.M. Lee, J.H. Lee, K.S. Seo, IEEE Electron Device Lett. 26 (11) (2005) 787.
[24] H. von Wenckstern, G. Biehne, R.A. Rahman, H. Hochmuth, M. Lorenz, M. Grundmann, Appl. Phys. Lett. 88 (9) (2006) 092102.
[25] J. Osvald, Z.J. Horvath, Appl. Surf. Sci. 234 (1–4) (2004) 349.
[26] E. Ayyildiz, H. Cetin, Zs.J. Horvath, Appl. Surf. Sci. 252 (2005) 1153.
[27] F.E. Jones, C.D. Hafer, B.P. Wood, R.G. Danner, M.C. Lonergan, J. Appl. Phys. 90 (2001) 1001.
[28] H.J. Im, Y. Ding, J.P. Pelz, W.J. Choyke, Phys. Rev. B 64 (7) (2001) 075310.
[29] R.C. Rossi, N.S. Lewis, J. Phys. Chem. B 105 (17) (2001) 12303.
[30] Y.P. Song, R.L. Van Meirhaeghe, W.H. Laflére, F. Cardon, Solid-State Electron. 29 (1986) 633.
[31] J.H. Werner, H.H. Güttler, J. Appl. Phys. 69 (1991) 1522.
[32] S. Chand, J. Kumar, J. Appl. Phys. 82 (1997) 5005; S. Chand, S. Bala, Appl. Surf. Sci. 252 (2005) 358; S. Chand, J. Kumar, Appl. Phys. A 65 (1997) 497.
[33] S. Zhu, R.L. Van Meirhaeghe, S. Forment, G. Ru, B. Li, Solid-State Electron. 48 (2004) 29.
[34] J. Osvald, J. Appl. Phys. 85 (3) (1999) 1935; E. Dobrocka, J. Osvald, Appl. Phys. Lett. 65 (1994) 575; J. Osvald, Solid-State Electron. 50 (2006) 228.
[35] M. Biber, A. Turut, J. Electron. Mater. 31 (12) (2002) 1362; M. Biber, C. Temirci, A. Turut, J. Vac. Sci. Technol. B 20 (1) (2002) 10; M. Biber, M. Cakar, A. Turut, J. Mater. Sci. Mater. Electron. 12 (2001) 575.
[36] R.T. Tung, Phys. Rev. B 45 (1992) 13509.

[37] J.P. Sullivan, R.T. Tung, M.R. Pinto, W.R. Graham, J. Appl. Phys. 70 (1991) 7403.
[38] S. Huang, B. Shen, M.J. Wang, F.J. Xu, Y. Wang, H.Y. Yang, F. Lin, L. Lu, Z.P. Chen, Z.X. Qin, Z.J. Yang, G.Y. Zhang, Appl. Phys. Lett. 91 (2007) 072109.
[39] A. Gümüş, A. Türüt, N. Yalçın, J. Appl. Phys. 91 (2002) 245.
[40] R.F. Schmitsdorf, T.U. Kampen, W. Mönch, J. Vac. Sci. Technol. B 15 (1997) 1221.
[41] W.P. Leroy, K. Opsomer, S. Forment, R.L. Van Meirhaeghe, Solid-State Electron. 49 (2005) 878.
[42] F.E. Cimilli, M. Saglam, A. Turut, Semicond. Sci. Technol. 22 (2007) 851.